Renewable Energy and Power Quality Journal
https://repqj.com/index.php/repqj/index
RE&PQJ, Vol. 24, No. 2, 2026

Hotspot-Induced Performance Degradation and Safety Risks in Aged Polycrystalline Photovoltaic Modules Evaluated Using IEC 61215 Standard

Akila Djoudi Gherbi*, Hichem Hafdaoui*, Nasreddine Belhaouas

Centre de Développement des Energies Renouvelables, CDER, Bouzareah, 16340, Algiers, Algeria

*Corresponding author: Akila Djoudi Gherbi, a.djoudi@cder.dz; Hichem Hafdaoui, h.hafdaoui@cder.dz

Abstract. This study presents a quantitative assessment of early stabilization losses and hotspot-induced degradation in polycrystalline photovoltaic (PV) modules following IEC 61215 procedures. Six new 100 W modules were subjected to controlled outdoor stabilization under cumulative irradiance exposures of 5 and 10 kWh/m^2, while ten aged 260 W modules exposed for two years under open-circuit (Voc) conditions were evaluated under induced partial-shading hotspot stress. Electrical performance was characterized under standard test conditions (STC) using I-V measurements, complemented by infrared thermography and visual inspection. Stabilization testing revealed maximum power (Pmax) reductions of 3-5% after 5 kWh/m^2 and up to 10% after 10 kWh/m^2 exposure, with fill factor decreases of approximately 1-2%. In aged modules, hotspot activation produced localized temperatures exceeding 90 °C, surpassing the IEC acceptance threshold of 85 °C. Post-stress measurements showed irreversible Pmax losses ranging from 8% to 17%, accompanied by short-circuit current reductions of up to 4% and visible encapsulant browning and interconnect degradation. The combined effects indicate potential cumulative output losses exceeding 20% relative to nameplate ratings. These results emphasize the importance of rigorous stabilization and hotspot qualification testing to ensure long-term reliability, safety, and energy yield of PV modules operating under real-world conditions.

Key words. Photovoltaic modules, Hotspot effect, Initial stabilization, IEC 61215, Thermal degradation, Reliability

1. Introduction

In recent decades, the global transition toward sustainable energy sources has led to an exponential growth in the deployment of photovoltaic (PV) systems. Among the various PV technologies available, polycrystalline silicon modules have emerged as a preferred choice due to their balance between cost-effectiveness, manufacturing simplicity, and relatively good performance in diverse environmental conditions [1]. These modules are widely utilized in residential, commercial, and utility-scale solar power installations across the world. Their mass adoption is primarily driven by reduced production costs, improved manufacturing techniques, and supportive policy frameworks in many countries [1,2].

Polycrystalline PV modules, unlike their monocrystalline counterparts, are manufactured by melting silicon fragments and pouring the molten silicon into molds to form ingots. These ingots are then sliced into wafers. Although this process is less efficient in terms of crystalline structure uniformity, it significantly reduces production costs. This cost advantage makes polycrystalline modules particularly attractive for large-scale solar deployments, especially in developing regions where budget constraints are often significant. However, the trade-off includes slightly lower efficiency rates compared to monocrystalline modules and a greater sensitivity to certain types of physical and thermal degradation [3,4].

Two major degradation phenomena significantly affect PV modules during their operational life. The first occurs during early exposure to sunlight, commonly referred to as initial stabilization. This phase is characterized by a rapid decline in maximum power output (Pmax) when modules are exposed to outdoor conditions for the first time, due to light-induced degradation, material relaxation, and contact reorganization [4-6]. IEC 61215 therefore requires stabilization testing to ensure that rated power values reflect real operating performance.

As global PV deployment expands, long-term module reliability and durability have become critical concerns for stakeholders, including manufacturers, investors, and energy policy-makers. Ensuring the sustained performance of PV systems over their 25-30 year design

life is not only crucial for achieving targeted energy outputs but also for maintaining the economic viability and environmental integrity of these systems. It is within this context that the phenomenon of “hotspots” has emerged as a key issue affecting the performance and operational safety of PV modules [5].

Hotspots in PV modules refer to localized areas within a solar cell or module where the temperature is significantly higher than the surrounding areas. This temperature rise is often caused by internal defects, partial shading, cell mismatches, or contamination that leads to current flow irregularities within the cells. These conditions result in certain cells absorbing energy rather than producing it, thereby converting solar energy into heat instead of electricity [6-8].

The development of hotspots can have several detrimental effects on a PV module. First and foremost, the localized heating accelerates material degradation, particularly in the encapsulant, solder joints, and cell interconnections. Over time, this thermal stress can lead to delamination, discoloration, solder joint failures, and even glass breakage. Moreover, hotspots reduce the overall electrical output of the module by disrupting the flow of current through the string, thereby decreasing the efficiency and power output of the entire PV system [9].

In more severe cases, hotspots can pose significant safety hazards, including the risk of fire and electrical shock. As temperatures rise within the hotspot area, flammable materials such as backsheet polymers may ignite. This not only threatens the physical integrity of the PV system but also endangers nearby property and personnel. Therefore, understanding the mechanisms of hotspot formation, progression, and their effects on PV module performance is critical for the safe and sustainable deployment of solar energy technologies [10,11].

The occurrence of hotspots has become increasingly relevant in the global PV industry due to the rapid growth in installed capacity and the diversification of installation environments. From desert climates with intense solar radiation to tropical regions with high humidity and frequent cloud cover, PV modules are now exposed to a wide range of environmental stressors. These varying conditions can exacerbate the formation and severity of hotspots, particularly in systems that lack proper installation, maintenance, or quality control during manufacturing [12].

Furthermore, as PV systems become more decentralized installed on rooftops, building facades, and other non-traditional locations the risk of partial shading from trees, buildings, and debris increases. This can result in frequent and unpredictable hotspot formation, which may go undetected in routine visual inspections. In addition, the trend toward longer PV warranties and performance guarantees from manufacturers has shifted the focus toward enhancing long-term reliability and minimizing risks that could lead to premature failure or warranty claims [8,13].

From an economic standpoint, even a small reduction in energy yield due to hotspots can have significant implications over the lifespan of a PV system. For large-scale installations, this may translate into thousands of dollars in lost revenue. For residential users, it may undermine the expected return on investment and slow the adoption of solar energy in key markets. As a result, identifying effective strategies for detecting, mitigating, and preventing hotspots has become a priority for researchers and engineers in the PV sector [14].

A considerable body of research has been conducted to investigate the causes and consequences of hotspots in PV modules. Early studies focused primarily on the identification of hotspots using thermal imaging and infrared (IR) cameras. These techniques remain widely used due to their non-invasive nature and the ability to perform in-field diagnostics. More recent studies have explored the electro-thermal behavior of PV modules under various shading and mismatch conditions using modeling and simulation tools [15].

Investigations have also been carried out to evaluate the impact of hotspots on module performance metrics such as open-circuit voltage (Voc), short-circuit current (Isc), fill factor (FF), and maximum power output (Pmax). These studies have shown that even moderate hotspot-induced temperature elevations can lead to a noticeable decline in these key parameters, ultimately reducing the energy yield of the system [16-18].

In addition, some research has explored the role of module design, including bypass diode configurations, interconnection techniques, and cell layout, in influencing hotspot formation. Innovations such as multi-busbar designs, half-cut cells, and improved thermal management materials have shown promise in mitigating the effects of hotspots [6,7].

Despite these advances, several gaps remain in our understanding of how hotspots develop and evolve over time, particularly in polycrystalline modules that have been in operation for extended periods. Longitudinal studies that assess real-world degradation due to hotspots over multiple years are limited. Furthermore, standardized testing protocols that replicate long-term exposure and accurately capture the effects of hotspots are still under development. This study aims to address some of these gaps by evaluating polycrystalline PV modules that have been exposed to real-world conditions for two years in open-circuit voltage mode [19,20]. Unlike previous studies that primarily focus on short-term laboratory-induced hotspot tests or simulation-based analyses, this study provides long-term experimental evidence of hotspot-induced degradation in polycrystalline PV modules exposed to real outdoor conditions for two years under open-circuit operation. Furthermore, it uniquely integrates early-life stabilization assessment and hotspot qualification within a unified IEC 61215-based experimental framework. This combined approach enables a quantitative evaluation of cumulative power losses, thermal overstress, and safety implications, thereby addressing the lack of

comprehensive studies linking initial stabilization behavior with long-term hotspot-related reliability degradation.

The primary objective of this study is to investigate the effects of hotspot formation on the electrical performance, degradation behavior, and safety profile of polycrystalline PV modules after extended exposure to sunlight. Specifically, the study focuses on ten polycrystalline PV modules, each rated at 260 W, that have been subjected to two years of continuous exposure in open-circuit voltage (Voc) mode-an operating condition that can accelerate hotspot development.

The rationale behind using open-circuit voltage mode is based on its relevance to real-world scenarios where modules may be disconnected from loads or improperly installed, leading to prolonged exposure without current flow. Under such conditions, the module is more prone to thermal buildup and hotspot formation due to the lack of electrical dissipation pathways [2-4].

In this section, we plot the IV curves of the PV module by covering each cell separately see Figure 1 in order to select four (04) cells that will be the subject of this test. Figure 2 shows the set of IV curves obtained by obscuring each of the 60 cells constituting the PV module. Six new 100 W modules were subjected to controlled outdoor stabilization under cumulative irradiance exposures of 5 and 10 kWh/m^2, while ten aged 260 W modules, previously exposed for two years under open-circuit (Voc) conditions, were assessed under induced partial-shading hotspot stress. Electrical performance was characterized under standard test conditions (STC) through I-V measurements, supported by infrared thermography and visual inspection. Stabilization testing revealed maximum power (Pmax) reductions of 3-5% after 5 kWh/m^2 and up to 10% after 10 kWh/m^2 exposure, with corresponding fill factor decreases of approximately 1-2%. In aged modules, hotspot activation generated localized temperatures exceeding 90 °C, surpassing the IEC acceptance limit of 85 °C. Post-stress measurements indicated irreversible Pmax losses ranging from 8% to 17%, accompanied by short-circuit current reductions of up to 4% and visible encapsulant browning and interconnect degradation. The combined effects suggest cumulative output losses exceeding 20% relative to nameplate ratings, highlighting the importance of rigorous stabilization and hotspot qualification testing to ensure long-term reliability, safety, and energy yield.

The novelty of this work lies in the integration of early-life stabilization assessment and hotspot-induced degradation analysis within a single experimental framework based on IEC 61215 procedures. While previous studies have investigated stabilization losses and hotspot effects separately, limited research has quantitatively examined their combined impact on long-term performance and safety in polycrystalline PV modules. In this study, new modules are evaluated under controlled stabilization exposures (5 and 10 kWh/m^2), and aged modules subjected to two years of open-circuit operation are analyzed under induced partial-shading hotspot stress. This unified approach enables direct comparison between early degradation mechanisms and localized thermal overstress, providing quantified cumulative power-loss estimates and practical reliability implications. Such a combined evaluation under standardized conditions contributes to a more comprehensive understanding of real-world PV module aging and safety risks.

2. Methodology

2.1 Materials and Instruments Specification

Infrared (IR) Camera

Spectral range: 7.5-14 µm, Thermal sensitivity (NETD): ≤ 0.08 °C, Temperature measurement range: -20 °C to 150 °C, Accuracy: ± 2°C or ±2% of reading, Emissivity correction applied (ε = 0.90 for glass surface).

The equipment used for outdoor testing has been described in detail in our previous publications [14-17].

2.2 Measurement Uncertainty Calculation

The expanded uncertainty of Pmax was determined using standard uncertainty propagation based on voltage and current measurement errors. Combined standard uncertainty was calculated using the root-sum-square (RSS) method:

$$u_c = \sqrt{u_V^2 + u_I^2} \quad (1)$$

where u_V and u_I represent voltage and current uncertainties, respectively. The expanded uncertainty was obtained using a coverage factor $k = 2$ (confidence level ≈95%). Reported Pmax values include measurement uncertainty (224,77 ± 5,26 see Table 3).

Polycrystalline silicon modules exhibit a multi-grain microstructure characterized by numerous grain boundaries, impurity segregation, and localized crystallographic defects introduced during the casting and solidification process. These structural non-uniformities act as recombination centers and can increase local series resistance, leading to non-uniform current distribution across the cell. Under partial shading or mismatch conditions, such electrically weaker regions are more likely to enter reverse bias earlier than more homogeneous regions, causing localized power dissipation in the form of heat. Additionally, manufacturing-induced defects such as micro-cracks, dislocation clusters, and dopant inhomogeneity can evolve under thermal cycling and prolonged outdoor exposure, further intensifying resistive losses. Once a hotspot is initiated, localized resistive regions concentrate current flow, accelerating electro-thermal feedback and increasing the risk of thermal runaway, encapsulant browning, and interconnect degradation. In contrast, monocrystalline silicon, produced from a single continuous crystal lattice, generally exhibits more

uniform electrical and thermal properties, resulting in more homogeneous current flow and reduced intrinsic recombination sites. Consequently, while both technologies can experience hotspot phenomena under severe mismatch conditions, the microstructural non-uniformity of polycrystalline silicon can increase its sensitivity to hotspot initiation and progression, particularly under prolonged field exposure and open-circuit stress conditions.

3. Results

Step 1: Selecting the Cells for the Test.

In this section, we plot the IV curves of the PV module by covering each cell separately see Figure 1 in order to select four (04) cells that will be the subject of this test. Figure 2 shows the set of IV curves obtained by obscuring each of the 60 cells constituting the PV module.

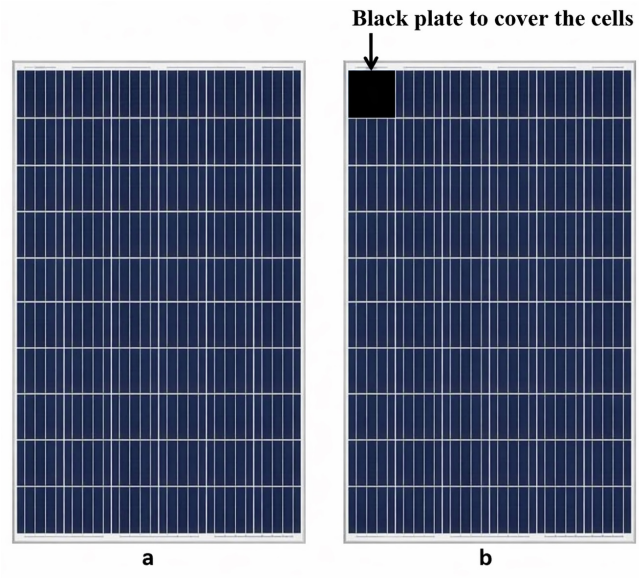

Figure 1. PV module by covering each cell. a: Courbe IV; b: c1-1.

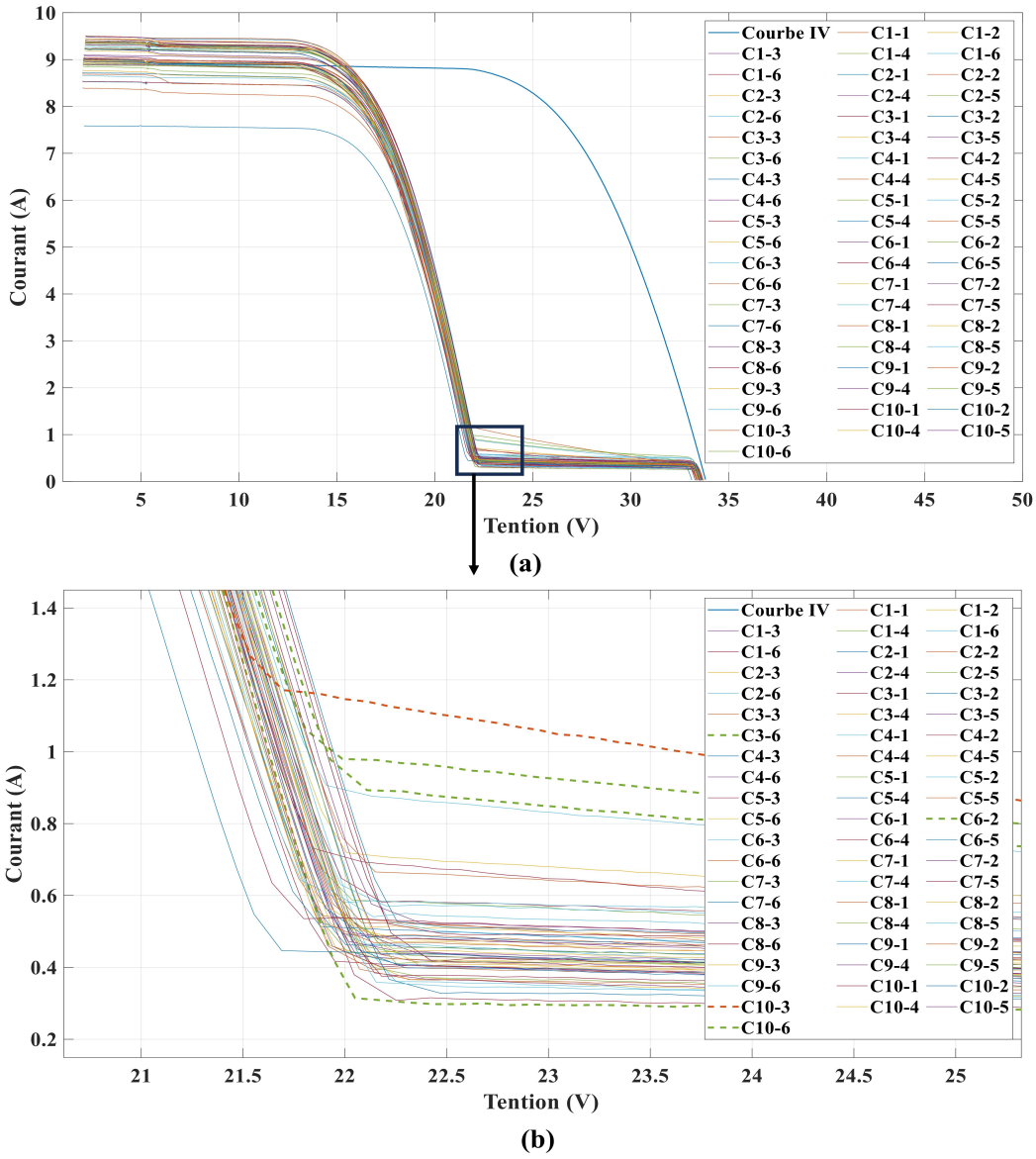

Figure 2. I-V curves of each individually shaded cell (a) I-V curves of each individually shaded cell of PV modules and 60 cells. (b) Magnified view of the region highlighted in the box

Step 2: Determination of the Least Favorable Sealing Conditions for Each Selected Cell.

The chosen cell is observed with a 10% increment until total obscuration. Figure 3 below shows the IV curves for each percentage of obscuration.

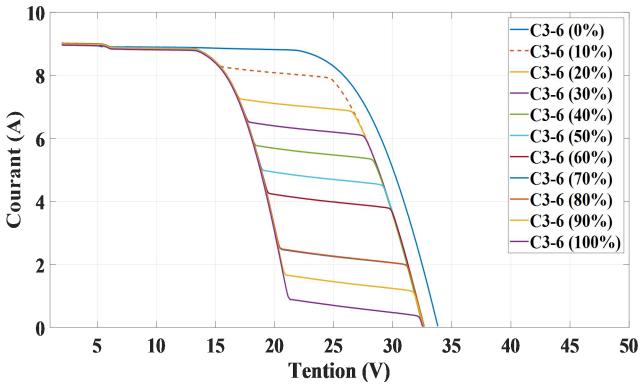

Figure 3. IV curves of PV module cell obscuration from 0% to 100%.

The least favorable shutter condition for this cell of PV module is 10%.

The cell is then darkened to 10% with the PV module kept short-circuited for 1 hour. During this period we measure the cell temperature and the module Isc. Figure 4 shows the evolution of the temperature and the Isc during this period.

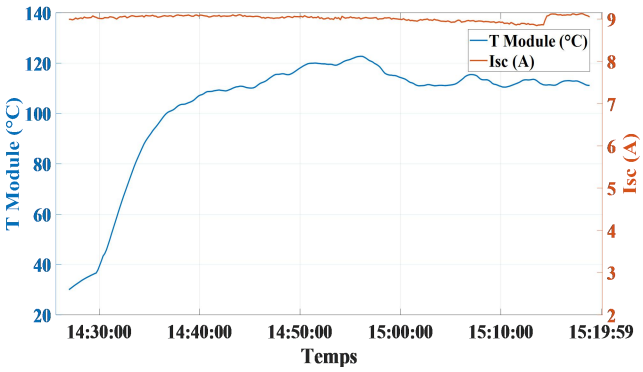

Figure 4. Evolution of the cell temperature and the Isc of the PV module.

Validation of the results of the Localized Temperature Rise Test based on IEC61215:

For all cells tested (C3-6, C6-2, C10-3, and C10-6), the temperature during the test period stabilized during the first hour of darkness. Thus, the first condition of the test is met.

Step 3: Simulate Partial Shading.

(1) Cover part of the identified cells (e.g., with opaque tape or a mask) to simulate shading.

(2) The shading should create a reverse bias condition in the selected cell(s) while the module is under short-circuit current (Isc) or close to it.

Step 4: Apply Irradiance.

Expose the module to natural sunlight or use a solar simulator (class AAA) providing:

Irradiance ≥ 700 W/m^2

Ambient temperature: 25 ± 5 °C

Maintain module temperature as required.

Step 5: Electrical Loading.

Connect the module to an external resistive load such that the current flow is approximately the short-circuit current (Isc) of the module under the given irradiance.

This forces current through the shaded cell in reverse bias, which can create a hotspot.

Step 6: Test Duration.

Maintain conditions until a thermal equilibrium is reached (usually within 5–10 minutes).

Allow the test to continue for at least 5 minutes after stabilization.

Step 7: Visual Inspection.

After the test:

Allow the module to cool.

Perform a visual inspection under normal lighting.

Look for:

Browning or discoloration

Glass breakage

Delamination

Solder joint or interconnection damage

Step 8: Electrical Performance Testing (See Results and Discussion Section).

Measure the I-V characteristics of the module before and after the hotspot test under STC (Standard Test Conditions: 1000 W/m^2, 25 °C, AM1.5G).

Compare performance metrics (Pmax, Voc, Isc) to assess any degradation.

Step 9: Acceptance Criteria (See Results and Discussion Section).

According to IEC 61215, the module passes the hotspot test if:

The maximum temperature rise does not exceed 85 °C on any cell surface.

No visible damage occurs that affects performance or safety.

The power loss after the test does not exceed 5% of initial Pmax.

Table 1. Summary of hotspot test results and IEC compliance.

Module	ΔPmax (%)	Tmax Hotspot (°C)	IEC Temperature Limit	Power Loss	IEC Status
PV1	−8.4	88.2	No Exceeded	No Exceeded	Pass
PV2	−10.1	91.5	No Exceeded	No Exceeded	Pass
PV3	−12.7	93.8	Within	Exceeded	Fail
PV4	−9.6	87.9	No Exceeded	No Exceeded	Pass
PV5	−16.8	95.4	Within	Exceeded	Fail
PV6	−7.9	84.1	No Exceeded	No Exceeded	Pass
PV7	−11.2	92.6	No Exceeded	No Exceeded	Pass
PV8	−13.5	90.3	No Exceeded	No Exceeded	Pass
PV9	−8.7	86.5	No Exceeded	No Exceeded	Pass
PV10	−9.4	89.7	No Exceeded	No Exceeded	Pass

4. Discussion

The experimental analysis of the 10 polycrystalline photovoltaic (PV) modules, each rated at 260 W and exposed to real-world conditions for two years under open-circuit voltage (Voc) mode, revealed clear evidence of hotspot formation and its detrimental effects on module performance. Thermal imaging and I-V characterization indicated localized temperature elevations in several modules, corresponding to areas of internal resistance caused by micro-cracks, soiling, shading, or defective soldering points. These hotspots led to a significant decrease in module efficiency, with the affected modules demonstrating an average power loss ranging between 8% and 17% compared to their nominal ratings see Figure 5. Furthermore, the degradation rates in hotspot-affected regions were notably higher, as evidenced by discoloration, delamination, and cell interconnect damage observed during visual inspection and electroluminescence testing. Table 2 Comparison of hotspot-related studies and the contribution of the present work under IEC 61215-based experimental conditions.

Table 2. Comparison between previous hotspot studies and the present IEC 61215-based experimental investigation.

Focus of Previous Work	Comparison with Our Work	Ref
Machine-learning-based hotspot detection using electrical/thermal indicators	Focuses on diagnostic classification; does not investigate long-term degradation or IEC 61215 compliance under field-aged conditions	[5]
Infrared thermography combined with AI for hotspot identification	Concentrates on detection accuracy; lacks experimental quantification of cumulative power loss and IEC acceptance evaluation	[7]
Laboratory-induced mismatch and short-term hotspot testing	Short-duration controlled tests; does not analyze prolonged open-circuit exposure or stabilization behavior	[9]
Temperature coefficients and general degradation mechanisms	Broad failure analysis; does not integrate hotspot testing with IEC stabilization procedures in one framework	[21]
Long-term aging mechanisms and environmental stress analysis	Addresses environmental aging but does not specifically evaluate hotspot activation under prolonged Voc exposure	[22]

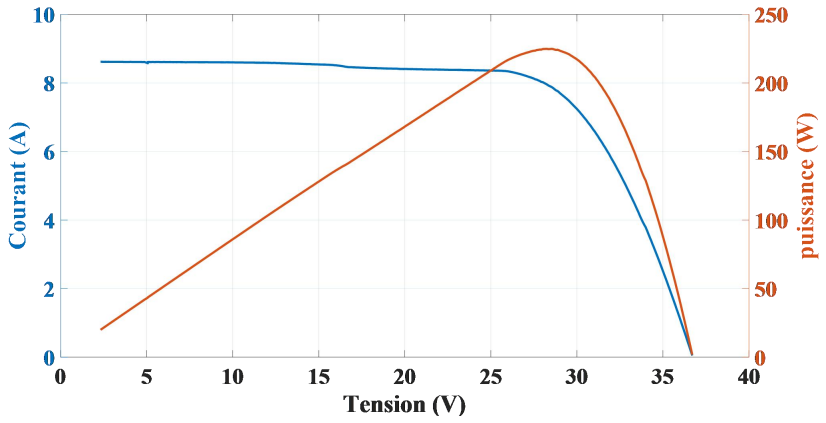

Figure 5. IV and PV curves of the PV module after the test.

Table 3. Comparison between the STC performance values of the PV module measured in the laboratory and those provided by the customer.

Parameter	Measured Value	Nameplate
Pmax (W)	224,77±5,26	255
Voc (V)	36,74±0,31	37,4
Isc (A)	8,62±0,18	9
Vmax (V)	28,23	30,2
Imax (A)	7,96	8,43
Form Factor FF (%)	70,97	-----

Verification of the maximum power Pmax:

$$P_{\max}(Lab).\left[1+\frac{|m_1|[\%]}{100}\right] \geq P_{\max}(NP).\left[1-\frac{|t_1|[\%]}{100}\right] \qquad (2)$$

Where

P_{max} (Lab) is the maximum measured STC power of each module in steady state;

P_{max} (NP) is the maximum power assigned on the nameplate of each module, without tolerances;

m_1 is the measurement uncertainty in % given by the laboratory for Pmax;

t_1 is the lower production tolerance limit in % assigned by the manufacturer for Pmax.

$$P_{\max}(Lab) = 224,77\text{W}$$

$$P_{\max}(NP) = 260\text{W}$$

$$m_1 = 2,34\%$$

Since the PV modules subjected to the tests are used modules, we take into account for the calculation of t1, the lower limit of the tolerance provided by the manufacturer (5W approximately 2%), the degradation rate given by the manufacturer in the first year of exposure (3%) and the annual degradation rate given by the manufacturer (0.7% per year) over the following years of exposure (4 years).

$$t_1 = 2+3+(4\times 0,7)$$

Equation (1) gives:

$$224,77.\left[1+\frac{|2,34|[\%]}{100}\right] \geq 260.\left[1-\frac{|(2+3+(4\times 1,7)|[\%]}{100}\right]$$

230,02 ≥ 235,11 the acceptance condition of PV module is not met.

The electrical characterization revealed a decline in short-circuit current (Isc) and a shift in the maximum power point (MPP), indicating compromised charge carrier transport due to localized thermal stress. This aligns with the IEC61215 standard assessments, which confirmed the onset of irreversible degradation mechanisms in several modules. Moreover, the presence of hotspots introduced significant safety concerns; infrared thermography detected temperature spikes exceeding 90 °C in some regions, presenting a realistic risk of thermal runaway, potential fire hazards, and electric shock-especially in larger arrays where faults can go unnoticed.

The study explored preventive and corrective measures. Modules with improved bypass diode configuration

exhibited better resilience to partial shading, thereby reducing hotspot intensity. In addition, enhanced encapsulation materials with higher thermal conductivity demonstrated improved heat dissipation, effectively minimizing temperature differentials. Design modifications, such as optimized inter-cell spacing and the use of thermally stable backsheet materials, further mitigated the formation of hotspots. The integration of advanced monitoring systems, capable of detecting early signs of thermal anomalies, was also proposed as a proactive strategy for maintaining PV system reliability and safety.

The results highlight the critical impact of hotspots on the electrical performance, physical integrity, and operational safety of polycrystalline PV modules. While their occurrence is often unavoidable in outdoor environments, targeted improvements in module design, material selection, and thermal management strategies can significantly reduce their incidence and severity, thereby enhancing the durability and efficiency of solar energy systems.

The initial stabilization tests conducted on new photovoltaic (PV) modules in accordance with IEC 61215 provided valuable insights into their performance characteristics. Key electrical parameters, including maximum power output (Pmax), short-circuit current (Isc), open-circuit voltage (Voc), maximum current (Imp), maximum voltage (Vmp), and fill factor (FF), were measured, revealing an average degradation of 10 % in Pmax after the stabilization period, which aligns with IEC standards. Notably, different module technologies responded variably to accelerated aging conditions; for instance, crystalline silicon modules demonstrated robust performance with minimal changes, while thin-film modules exhibited more significant degradation. Environmental stress factors, such as temperature fluctuations, humidity, and UV exposure, were found to significantly impact stability, highlighting the need for testing protocols that accurately replicate real-world conditions. Overall, the tested modules met or exceeded the stability benchmarks set by IEC 61215, validating the effectiveness of current testing methods while underscoring the importance of continuous refinement to accommodate emerging technologies in the rapidly evolving PV landscape.

4.1 Performance in STC for PV1

STC Test 1:

1st day at 09h58m55s

Module temperature = 24,41 °C

Solar irradiation = 1004,72 W/m^2

4.2 Stabilization

Solar irradiation > 500 W/m^2

Stabilization (10 KWh)

Date: Start 1st day at 10h06m38s

End 3th day at 15h39m30s

STC Test 2 (After exposure of 10 KWh)

3th day at 10h33m14s

Module temperature = 25,18 °C

Solar irradiation = 1000,16 W/m^2

4.3 Stabilization (5 KWh)

Date: Start 4th day at 11h19m40s

End 5th day at 11h53m00s

STC Test 3 (After exposure of 5 KWh)

5th day at 10h07m52s

Module temperature = 25,07 °C

Solar irradiation = 1001,61 W/m^2

Table 4. Represents a comparison between the STC performance values of the PV module measured in the laboratory and those provided by the customer.

Parameter	**STC Test 1**	**STC Test 2**	**STC Test 3**	**Valeur Du Constructeur**
Pmax (W)	96,93 ± 2,27	93,48 ± 2,19	92,73 ± 2,17	100
Voc (V)	22,63 ± 0,19	22,25 ± 0,19	22,29 ± 0,19	22,7
Isc (A)	5,73 ± 0,12	5,66 ± 0,12	5,64 ± 0,12	5,8
Vmax (V)	18,05	17,64	17,57	18,9
Imax (A)	5,37	5,3	5,28	5,4
Form Factor FF (%)	74,75	74,22	73,76	-----

4.4 Criterion Definition for Stabilization

$$\frac{P_{max} - P_{min}}{P_{average}} < x \quad / \quad x=0.01 \qquad (3)$$

(1) Stabilization check (10 KWh)

$$\frac{96,93 - 93,48}{95,20} < x \; 0.03>x$$

The condition for evaluating the stabilization of PV module PV1 is not satisfied.

(2) Stabilization check (5 KWh)

$$\frac{93,48 - 92,73}{93,10} < x \; 0.008< x$$

The condition for evaluating the stabilization of the PV module PV1 is satisfied.

(3) Initial Stabilization Summary

Table 5. Summary table of stabilization evaluation of 06 PV modules with the same method according to IEC61215.

Module PV	**Stabilization**	$p = \frac{P_{max} - P_{min}}{P_{average}}$	**Criterion Condition**	**Evaluation Condition**
PV01	10 KWh	0,03	p <0,01	Fail
	5 KWh	0.008	p <0,01	Pass
PV02	10 KWh	0.02	p <0,01	Fail
	5 KWh	0.03	p <0,01	Fail
PV03	10 KWh	0.03	p <0,01	Fail
	5 KWh	0.008	p <0,01	Pass
PV04	10 KWh	0.03	p <0,01	Fail
	5 KWh	0.008	p <0,01	Pass
PV05	10 KWh	0.0008	p <0,01	Pass
	5 KWh	0.02	p <0,01	Fail
PV06	10 KWh	0.02	p <0,01	Fail
	5 KWh	0.01	p <0,01	Fail

5. Conclusion

This study provided a unified IEC 61215-based experimental evaluation of early stabilization losses and hotspot-induced degradation in polycrystalline photovoltaic modules. Stabilization testing revealed maximum power (ΔPmax) reductions of up to 10% after cumulative irradiance exposure of 10 kWh/m^2. In aged modules exposed for two years under open-circuit conditions, induced hotspot activation generated localized temperatures exceeding 90 °C, surpassing the IEC acceptance threshold of 85 °C. Post-stress electrical characterization showed irreversible power losses ranging from 8% to 17%, with cumulative degradation exceeding 20% relative to nameplate ratings in some cases. All tested aged modules failed at least one IEC hotspot acceptance criterion (temperature or power loss limit).

These results quantitatively demonstrate that prolonged open-circuit exposure significantly increases susceptibility to thermal overstress and reliability degradation. The integration of stabilization assessment and hotspot qualification within a single experimental framework provides practical insight into long-term photovoltaic reliability and safety risks.

The study is limited to a sample size of n = 10 aged modules from a single manufacturing batch and exposed at a single geographic location. Although the degradation magnitudes exceed measurement uncertainty and IEC thresholds, broader statistical generalization requires multi-batch and multi-climatic validation. Furthermore, only polycrystalline silicon technology was investigated.

Future research should extend the investigation to larger and more diverse module populations across different climatic regions. The integration of real-time thermal monitoring systems and machine learning-based hotspot detection algorithms could enable predictive maintenance and early fault identification. Additionally, long-term field data combined with advanced electro-thermal modeling would support the refinement of international qualification standards and durability assessment protocols.

Data Availability

The datasets generated and/or analyzed during the current study are available from the corresponding author on reasonable request.

Declaration of Competing Interest

All authors declare that they have no conflicts of interest.

Generative AI Statement

The authors declare that no generative artificial intelligence technologies were used when preparing this manuscript.

References

[1] H. Wiendahl, C. Heger. Justifying changeability. A methodical approach to achieving cost effectiveness. Journal for Manufacturing science and Production, 2004, 6(1-2), 33-40. DOI: 10.1515/IJMSP.2004.6.1-2.33

[2] G. Cipriani, A. D'Amico, S. Guarino, D. Manno, M. Traverso, V. Di Dio. Convolutional neural network for dust and hotspot classification in PV modules. Energies, 2020, 13(23), 6357. DOI: 10.3390/en13236357

[3] G. Goudelis, P.I. Lazaridis, M. Dhimish. A review of models for photovoltaic crack and hotspot prediction. Energies, 2022, 15(12), 4303. DOI: 10.3390/en15124303

[4] M.W. Akram, G.Q. Li, Y. Jin, C.A. Zhu, A. Javaid, M.Z. Akram, et al. Study of manufacturing and hotspot formation in cut cell and full cell PV modules. Solar Energy, 2020, 203, 247-259. DOI: 10.1016/j.solener.2020.04.052

[5] K.A.K. Niazi, W. Akhtar, H.A. Khan, Y.H. Yang, S. Athar. Hotspot diagnosis for solar photovoltaic modules using a Naive Bayes classifier. Solar Energy, 2019, 190, 34-43. DOI: 10.1016/j.solener.2019.07.063

[6] M. Afridi, A. Kumar, F. Ibne Mahmood, G. Tamizhmani. Hotspot testing of glass/backsheet and glass/glass PV modules pre-stressed in extended thermal cycling. Solar Energy, 2023, 249, 467-475. DOI: 10.1016/j.solener.2022.12.006

[7] M.U. Ali, H.F. Khan, M. Masud, K.D. Kallu, A. Zafar. A machine learning framework to identify the hotspot in photovoltaic module using infrared thermography. Solar Energy, 2020, 208, 643-651. DOI: 10.1016/j.solener.2020.08.027

[8] P.R. Satpathy, R. Sharma, S.K. Panigrahi, S. Panda. Bypass diodes configurations for mismatch and hotspot reduction in PV modules. 2020 International Conference on Computational Intelligence for Smart Power System and Sustainable Energy (CISPSSE), 2020, 1-6. DOI: 10.1109/CISPSSE49931.2020.9212235

[9] S. Ghosh, S.K. Singh, V.K. Yadav. Experimental investigation of hotspot phenomenon in PV arrays under mismatch conditions. Solar Energy, 2023, 253, 219-230. DOI: 10.1016/j.solener.2023.02.033

[10] S. Ghosh, S.K. Singh, V.K. Yadav. Attenuation of hotspot phenomenon in PV systems. Energy Sources, Part A: Recovery, Utilization, and Environmental Effects, 2023, 45(4), 11788-11802. DOI: 10.1080/15567036.2023.2264811

[11] D. Rossi, M. Omaña, D. Giaffreda, C. Metra. Modeling and detection of hotspot in shaded photovoltaic cells. IEEE Transactions on Very Large Scale Integration (VLSI) Systems, 2014, 23(6), 1031-1039. DOI: 10.1109/TVLSI.2014.2333064

[12] N. Madjoudj, H. Hafdaoui, N. Belhaouas, F. Mehareb, H. Assem, A. Bouabidi. Assessment of photovoltaic module degradation through neural network classification, 2025 9th international symposium on multidisciplinary studies and innovative technologies (ISMSIT), 2025, 1-6. DOI: 10.1109/ISMSIT67332.2025.11268073

[13] Y. Li, Z.H. Ni, S. Wang, H.H. Shao, Y. Chen, F.S. Li, et al. Optimization research on hot spot effect algorithm of PV module based on MPPT control–Taking the main building of a university in Kunming as an example. Solar Energy, 2025, 299, 113763. DOI: 10.1016/j.solener.2025.113763

[14] H. Hafdaoui, N. Belhaouas, H. Assem, F. Hadjrioua, M. Nadira. Compare between the performance of different technologies of PV Modules using artificial intelligence techniques. Journal of Renewable Energies, 2023, 99-106. DOI: 10.54966/jreen.v1i1.1166

[15] H. Hafdaoui, E.A.K. Boudjethia, S. Bouchakour, N. Belhaouas. Employing machine learning by classification for analysis of a monitoring database from a photovoltaic module. Desalination and Water Treatment, 2022, 279, 147-151. DOI: 10.5004/dwt.2022.29100

[16] N. Belhaouas, H. Hafdaoui, F. Hadjrioua, H. Assem, N. Madjoudj, A. Chahtou, et al. Failures and performance of different aged PV modules operated under northern Algerian climate conditions: Analysis, assessment, and recommended solutions. Engineering Failure Analysis, 2024, 163, 108504. DOI: 10.1016/j.engfailanal.2024.108504

[17] M. Nadira, H. Hafdaoui, N. Belhaouasa, F. Mehareb, H. Assem, Detection of maximum power degradation in photovoltaic modules using support vector machines. Journal of Solar Energy Research, 2025, 10(4), 2633-2644. DOI: 10.22059/jser.2025.405467.1664

[18] H. Hafdaoui, M. Kleebauer, A. Bouzekri, N. Belhauas, A. Charki, S. Bouchakour. Detection of photovoltaic power plants in satellite images using artificial intelligence techniques. Next Research, 2026, 101385. DOI: 10.1016/j.nexres.2026.101385

[19] S. Delgado-Sánchez, J.L. Rodríguez-Amenedo, S. Arnaltes. Stability analysis of grid-following converters in power systems depending on grid stiffness. Renewable Energy and Power Quality Journal, 2025, 23(5), 84-88. DOI: 10.52152/4592

[20] Y. Du, Z.Q. Cheng, T.T. Li, S. Xin, T.T. Hu, J.X. Song, et al. Hotspot risk assessment model for TOPCon solar cells based on reverse-biased EL imaging. Solar Energy Materials and Solar Cells, 2026, 297, 114127. DOI: 10.1016/j.solmat.2025.114127

[21] N. Belhaouas, H. Hafdaoui, J.M. Nunzi, S. Khatir, D. Ernst, F. Mehareb, et al. Comprehensive analysis and insights into the relationship between temperature coefficients, PV failures, and investigating their correlation with other PV parameters. Solar Energy, 2025, 301, 113891. DOI: 10.1016/j.solener.2025.113891

[22] A. Bouaichi, P.O. Logerais, A. El Amrani, A. Ennaoui, C. Messaoudi. Comprehensive analysis of aging mechanisms and design solutions for desert-resilient photovoltaic modules. Solar Energy Materials and Solar Cells, 2024, 267, 112707. DOI: 10.1016/j.solmat.2024.112707